

Particle Behavior in Thermal Plasmas¹

E. Pfender²

Received February 10, 1988; revised March 4, 1988

In this overview, effects exerted on the motion and on heat and mass transfer of particulates injected into a thermal plasma are discussed, including an assessment of their relative importance in the context of thermal plasma processing of materials. Results of computer experiments are shown for particle sizes ranging from 5–50 μm , and for alumina and tungsten as sample materials. The results indicate that (i) the correction terms required for the viscous drag and the convective heat transfer due to strongly varying properties are the most important factors; (ii) noncontinuum effects are important for particle sizes $<10 \mu\text{m}$ at atmospheric pressure, and these effects will be enhanced for smaller particles and/or reduced pressures; (iii) the Basset history term is negligible, unless relatively large and light particles are considered over long processing distances; (iv) thermophoresis is not crucial for the injection of particles into thermal plasmas; (v) turbulent dispersion becomes important for particle $<10 \mu\text{m}$ in diameter; and (vi) vaporization describes a different particle heating history than that of the evaporation process which, however, is not a critical control mechanism for interphase mass transfer of particles injected into thermal plasmas.

KEY WORDS: Thermal plasmas; heat, mass, and momentum transfer; material processing; overview.

1. INTRODUCTION

This overview is concerned with heat, mass, and momentum transfer which particulates experience in a thermal plasma flow. This aspect is extremely important for material processing in thermal plasmas, including extractive metallurgy, plasma deposition, plasma synthesis and densification, and for plasma decomposition (toxic waste). Thermal plasmas

¹ Presented at the EPRI Exploratory Research Group Workshop on Research Opportunities for Plasma Processing, December 1–3, 1987, Palo Alto, California.

² Department of Mechanical Engineering, University of Minnesota, Minneapolis, Minnesota 55455.

with temperatures in the order of 10^4 K provide extremely high heating rates for injected materials as well as high quench rates for particles leaving the hot plasma. The latter aspect is of particular importance for plasma synthesis and for rapid solidification processes. Because of the high temperatures which are characteristic for thermal plasma reactors, the required processing time becomes very short, and this translates into relatively small reactors with high throughput rates.

In general, thermal plasma reactors are highly heterogeneous systems with large temperature and velocity variations. Over a distance of 10 mm, for example, the temperature may drop from 15,000 K to almost room temperature, or the velocity may drop from 500 m/s to almost zero. In such systems, the injected particles must pass through the hottest region in the plasma with maximum possible exposure to complete the desired physical or chemical processes. In some applications, fast acceleration of particles in the plasma is desirable so that they accumulate high velocities before impinging on a target.

One of the key factors for satisfying these requirements is the control of the particle trajectories and of the heat and mass transfer between particles and plasmas. In spite of increasing efforts over the past 10 years, understanding of the interaction of particulate matter with thermal plasmas still remains incomplete.

In the first part of this survey, thermal plasma properties will be reviewed with emphasis on those properties which exert an immediate effect on particle motion and on heat and mass transfer. In the second part, particle motion will be considered, neglecting thermal effects. And the last part will focus on particle heat and mass transfer. Both the second and the last parts will include an assessment of the relative importance of the various effects involved in particle heat, mass, and momentum transfer.

2. PROPERTIES OF THERMAL PLASMAS

Different types of thermal plasma reactors are feasible depending on the plasma generation process. Frequently, thermal plasmas are produced either by high-intensity arcs or by inductively coupled high-frequency (rf) discharges. The former includes operation in the transferred and nontransferred mode. In the case of nontransferred arcs, the useful plasma consists of a decaying plasma jet or plasma flame. Although the design and power level of thermal plasma reactors may vary over a wide range, such plasma reactors reveal a number of common features.

The thermodynamic state of the plasma in such reactors approaches local thermodynamic equilibrium (LTE) with temperatures typically in the order of 10^4 K in the current-carrying ("active") part of the plasma. In

contrast, plasma jets and plasma tail flames (field-free or “passive” plasmas) represent rapidly decaying plasmas with correspondingly decreasing temperatures. Another common feature of thermal plasma reactors is the relatively high velocity of the plasma, ranging from $10\text{--}10^2$ m/s or even 10^3 m/s. In addition to the flow due to the material throughout (particulate matter is usually injected with carrier gases) and/or the gas flow required for stabilizing the discharge, the discharge itself may produce substantial flows. Typical examples are self-induced flows in high-intensity arcs, first described by Maecker.⁽¹⁾

The plasma composition for a given gas or gas mixture in the reactor is only a function of the temperature, provided that LTE exists in the plasma. As an example, Fig. 1 shows the composition of a nitrogen plasma at atmospheric pressure. The plasma enthalpy is strongly affected by the plasma

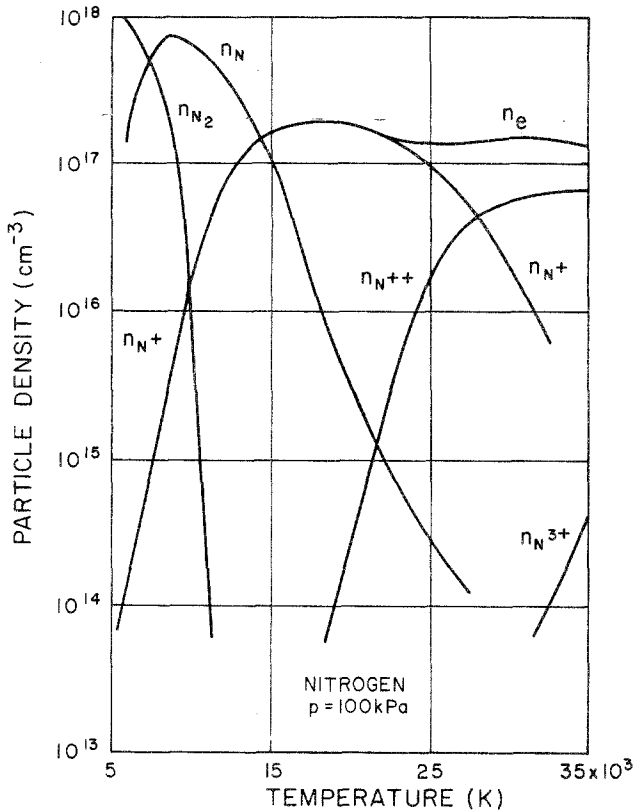


Fig. 1. Equilibrium composition of a nitrogen plasma.

composition as shown in Fig. 2. The presence of molecular species in the plasma gives rise to substantially higher enthalpies at a given temperature.

For a basic understanding of the behavior of particulate matter injected into a thermal plasma, it is necessary to know the conditions to which the particles will be exposed. Besides the already-mentioned conditions of temperatures, enthalpies, velocities, and plasma composition, plasma transport properties which depend on these conditions may affect heat and momentum transfer between the plasma and particulate matter. At this point it should be mentioned that small percentages of low ionization potential materials may have a substantial effect on some of the transport coefficients.^(2,3) "Contamination" of plasmas with such low ionization potential species is almost inevitable in plasma processing of particulate matter.

Finally, deviations from LTE in the plasma should be mentioned which cannot be neglected, in particular close to confining walls and electrodes. Figure 3 shows a typical example of such deviations in the fringes of a wall-stabilized arc.⁽⁴⁾ Even in the bulk of the plasma, the existence of LTE is rather the exception than the rule.⁽⁵⁾ Whether or not such deviations from LTE will substantially affect heat and momentum transfer to particles in the condensed phase, still remains a matter of speculation.

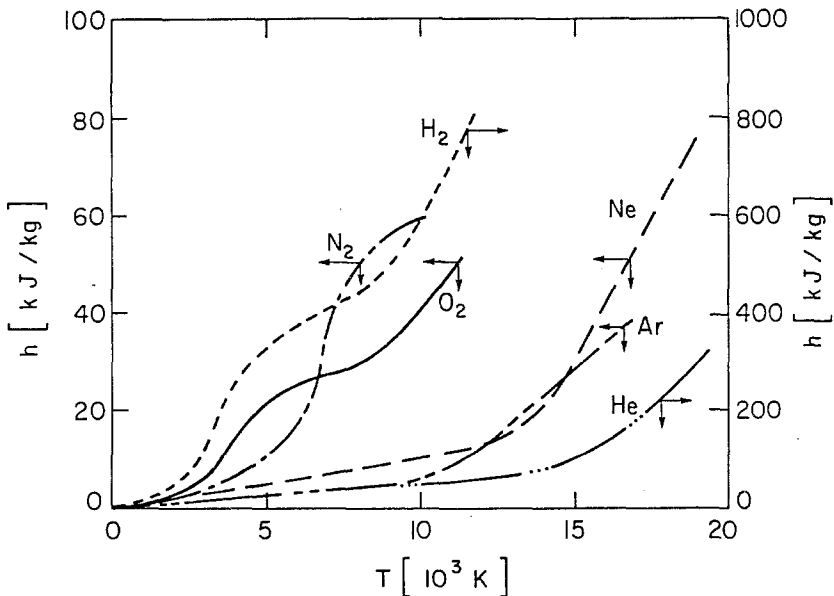


Fig. 2. Enthalpy of some monatomic and diatomic plasma gases.

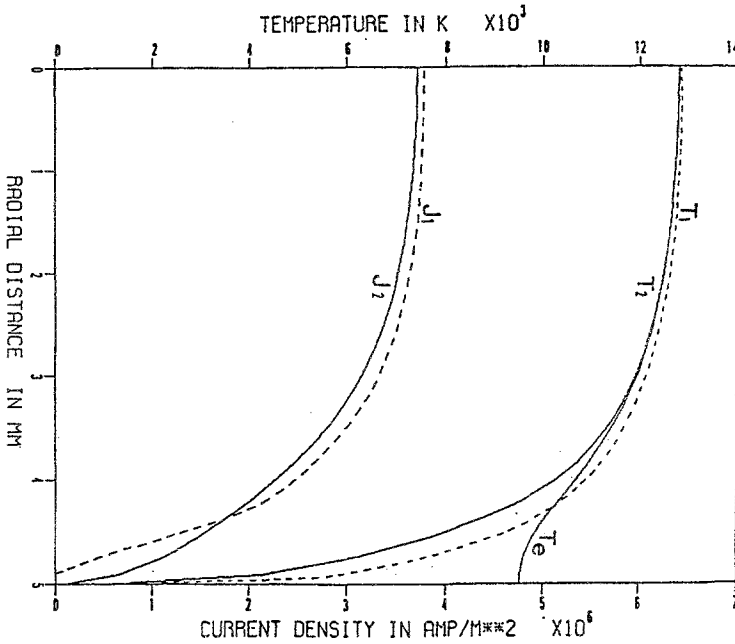


Fig. 3. Temperature and current density distributions in a fully developed argon arc at 1 atm and 200 A; 1 refers to 1-T model, and 2 refers to 2-T model.

3. PARTICLE MOTION IN THERMAL PLASMAS

In general, a number of effects, as shown in Table I, may be responsible for particle motion in a thermal plasma. In this section, particle motion will be considered without taking thermal effects into account.

Using a force balance, the equation of motion of a particle injected into a plasma may be established^(6,7)

$$\vec{F} = m\vec{a} = \vec{F}_D + \vec{F}_p + \vec{F}_a + \vec{F}_B + \vec{F}_{r1} + \vec{F}_{r2} + \vec{F}_{r3} + \vec{F}_e \tag{1}$$

Table I. Effects Involved in Particle Dynamics in a Thermal Plasma

-
1. Modified viscous drag due to strongly varying plasma properties
 2. Thermophoresis
 3. Noncontinuum effects
 4. Basset history term
 5. Turbulent dispersion
 6. Particle shapes
 7. Evaporation
 8. Particle charging
 9. Combination of above effects
-

where \vec{F} represents inertia, \vec{F}_D the viscous drag force, \vec{F}_p the pressure gradient term, \vec{F}_a the added mass term, \vec{F}_B the Basset history term, \vec{F}_{r_1} the top spin effect due to rotation of a particle in the velocity gradient of the fluid, \vec{F}_{r_2} the effect of rotation about an axis perpendicular to the direction of relative motion, \vec{F}_{r_3} the effect of rotation about an axis parallel to the direction of relative motion, and \vec{F}_e represents external forces (gravitational, electric, magnetic, etc.).

In a thermal plasma flow, the plasma density is rather low compared to the density of particulate matter. Therefore, all terms with exception of the viscous drag and the potential forces may be neglected.^(6,7) The Basset history term, however, may play a significant role in thermal plasma processing⁽⁸⁾ if highly decelerated flows are involved.

In addition to the terms in Eq. (1), thermophoresis and turbulence effects must be considered. Thermophoresis effects have been associated with observations of particles bouncing off plasmas. Turbulence effects (which have been qualitatively discussed in ref. 8) give rise to a certain random dispersion of the particle trajectories.

Considering typical plasma reactors for thermal plasma processing, external forces may be neglected. Thus, in the following only those terms listed in Eq. (2) will be considered in addition to turbulence effects, i.e.,

$$\vec{F} = \vec{F}_D + \vec{F}_B + \vec{F}_{TH} \quad (2)$$

where \vec{F}_{TH} represents thermophoresis.

3.1. Viscous Drag Force

Due to the small size (5–100 μm) of particles used in thermal plasma processing, the drag force exerted on a particle gives rise to a creeping flow situation. Different semiempirical relations for determining steady state, constant property drag coefficients ($\text{Re} < 100$) exist in the literature. A simple form⁽¹⁰⁾ will be adopted, i.e.,

$$C_D = \frac{24}{\text{Re}} + \frac{6}{1 + \sqrt{\text{Re}}} + 0.4 \quad (3)$$

This equation, however, does not apply to a particle moving in a thermal plasma. The Basset history term, variable property effects, and noncontinuum effects must be included. These effects will be discussed in the following.

3.2. Variable Property Effects

The temperature of a hot gas flowing over a sphere drops drastically in the boundary layer, and consequently there are property variations within

the boundary layer. Under such conditions, constant property equations are still valid but with properties corresponding to the film temperature. This approximation, however, is not valid for plasma flow. Table II shows some results of pertinent calculations which indicate that there are still large differences between film temperature approximations and those simulating the actual situation by numerical computations. Therefore, additional correction factors are needed. Two correction factors have been proposed.^(8,11)

According to ref. 8:

$$\rho_f C_{D_{VP}} = \rho_\infty C_{D_f} \left(\frac{\nu_f}{\nu_\infty} \right)^{0.15} \quad (4)$$

where ρ_f is the density corresponding to the film temperature T_f , ρ_∞ is the density corresponding to the free stream temperature, C_{D_f} is a coefficient derived from conventional expressions based on film temperature properties, $C_{D_{VP}}$ is a corrected drag coefficient associated with the use of ρ_f ; ν_f and ν_∞ are the kinematic viscosities corresponding to the film and free stream temperature, respectively.

Table II. Drag Coefficients Calculated by Different Methods for an Argon Plasma Flow over a Sphere

Case ^a	Re approach	0.1	1.0	10.0	20.0	50.0
1	Simulation ^b	100.8	15.4	2.9	1.8	1.0
	Film temp. ^c	100.6	12.3	2.4	1.6	1.1
	Lee <i>et al.</i> ^d	115.6	14.2	2.7	1.9	1.2
	Lewis and Gauvin ^e	146.1	17.9	3.4	2.4	1.6
2	Simulation	151.9	17.6	3.3	2.1	1.2
	Film temp.	112.9	13.7	2.5	1.7	1.1
	Lee <i>et al.</i>	136.9	16.6	3.1	2.1	1.4
	Lewis and Gauvin	164.5	19.9	3.7	2.5	1.7
3	Simulation	199.9	22.4	4.2	2.6	1.4
	Film temp.	137.6	16.2	2.9	1.9	1.2
	Lee <i>et al.</i>	202.3	23.9	4.2	2.8	1.8
	Lewis and Gauvin	226.8	26.8	4.7	3.2	2.0

^a Case 1: $T_\infty = 4000$ K and $T_w = 1000$ K; Case 2: $T_\infty = 10,000$ K and $T_w = 2500$ K; Case 3: $T_\infty = 12,000$ K and $T_w = 3000$ K.

^b Simulation: Numerical simulation by Lee.⁽¹²⁾

^c Film temp.: Approximation by Eq. (3) with film temperature properties.

^d Lee *et al.*⁽¹¹⁾: Correction of film temperature approximation by Eq. (5).

^e Lewis and Gauvin⁽⁸⁾: Correction of film temperature approximation by Eq. (4).

In ref. 11 another correction factor has been proposed, based on computational studies, i.e.,

$$C_{D_{VP}} = C_{D_f} \left(\frac{\rho_\infty \mu_\infty}{\rho_w \mu_w} \right)^{-0.45} \quad (5)$$

where ρ_w is the density and μ_w is the viscosity, both corresponding to the wall temperature of the sphere.

It is difficult to judge the validity of these two proposed correction factors, because no experimental data are available for comparison. With a few exceptions, the difference between the data^(8,11) are within 25% (see Table II). Since the data of ref. 11 were fitted to the computational results, Eq. (5) will be used as drag coefficient since it incorporates effects of strongly varying plasma properties.

3.3. Noncontinuum Effects

The mean free path lengths of the plasma constituents in thermal plasmas are in the order of μm at atmospheric pressure. Particles used in thermal plasma synthesis (1–10 μm) are almost of the same order of magnitude. Therefore, the continuum approach is no longer valid in this situation and modifications become necessary. Similar or even more severe conditions will be experienced in the case of plasma spraying in soft vacuum ($p = 50$ torr), where particles are typically larger, but the mean free path lengths are also longer.

In ref. 13 the importance of noncontinuum effects has been pointed out in the Knudsen number regime $10^{-2} < \text{Kn} < 1$ (the Knudsen number is defined as $\text{Kn} = \lambda/D_p$ with λ as the molecular mean free path and D_p as the particle diameter). A correction term for the drag coefficient has been proposed,⁽¹⁴⁾ i.e.,

$$C_{D_{\text{slip}}} = C_{D_{\text{con}}} \left[\frac{1}{1 + \left(\frac{2-a}{a} \right) \left(\frac{\gamma}{1+\gamma} \right) \frac{4}{\text{Pr}_w} \text{Kn}^*} \right]^{0.45} \quad (6)$$

where a is the thermal accommodation coefficient, γ the specific heat ratio, Pr_w the Prandtl number of the gas at the surface temperature of the sphere, and Kn^* the Knudsen number based on an effective mean free path length (see next section).

The validity of Eq. (6) cannot be proven, because of the lack of a basis for comparison. So far, it is the only available correction specifically proposed for plasma flows.

Conventionally, an expression proposed by Phillips⁽¹⁵⁾ is used to describe noncontinuum effects in the transitional range.

Figure 4 shows a comparison of these two correction terms, indicating that there is no significant difference between these two differently derived correction factors. Therefore, Eq. (6) will be used for describing noncontinuum effects in the case of thermal plasma flows and for Knudsen numbers in the range $10^{-2} < Kn < 1$.

Combining the results of this and the previous subsection, a general expression is proposed for the drag coefficient, i.e.,

$$C_D = C_{D_f} \cdot f_1 \cdot f_2 \tag{7}$$

where C_{D_f} may be calculated from Eq. (3) based on film temperature properties, and

$$f_1 = \left(\frac{\rho_\infty \mu_\infty}{\rho_w \mu_w} \right)^{-0.45} \tag{8}$$

is an additional correction factor for strongly varying plasma properties, and

$$f_2 = \left[1 + \left(\frac{2-a}{a} \right) \left(\frac{\gamma}{1+\gamma} \right) \frac{4}{Pr_w} Kn^* \right]^{-0.45} \tag{9}$$

incorporates noncontinuum effects.

Figures 5 and 6 show some results of the acceleration caused by viscous drag forces calculated from Eqs. (7-9) and expressed in units of G (acceleration due to gravity). The plasma flow conditions are uniform and are

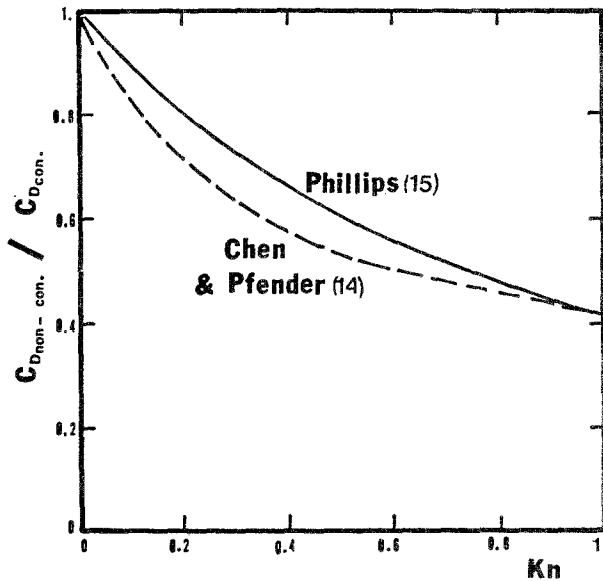


Fig. 4. Comparison between proposed correction factors of refs. 14 and 15 for modeling of noncontinuum effects on the drag coefficient.

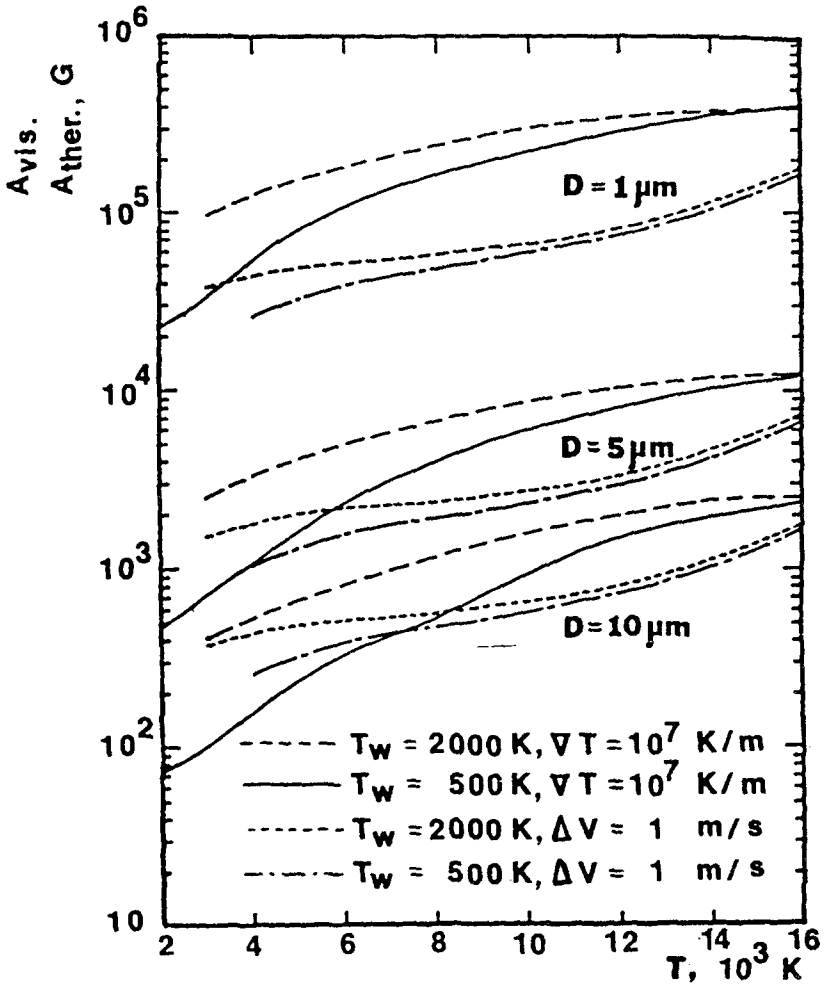


Fig. 5. Acceleration caused by viscous drag and by thermophoresis (alumina).

specified in terms of temperature. The relative velocity is assumed to be 1 m/s. Thermophoresis effects are also shown in these figures and they will be discussed later on. The results presented in these two figures can be used for other materials and other particle sizes as well, because there are three similarity rules. In a first approximation, the magnitude of acceleration exerted on a spherical particle is

- (i) inversely proportional to the particle density,
- (ii) inversely proportional to the square of the diameter of the particle,
- (iii) proportional to the relative velocity.

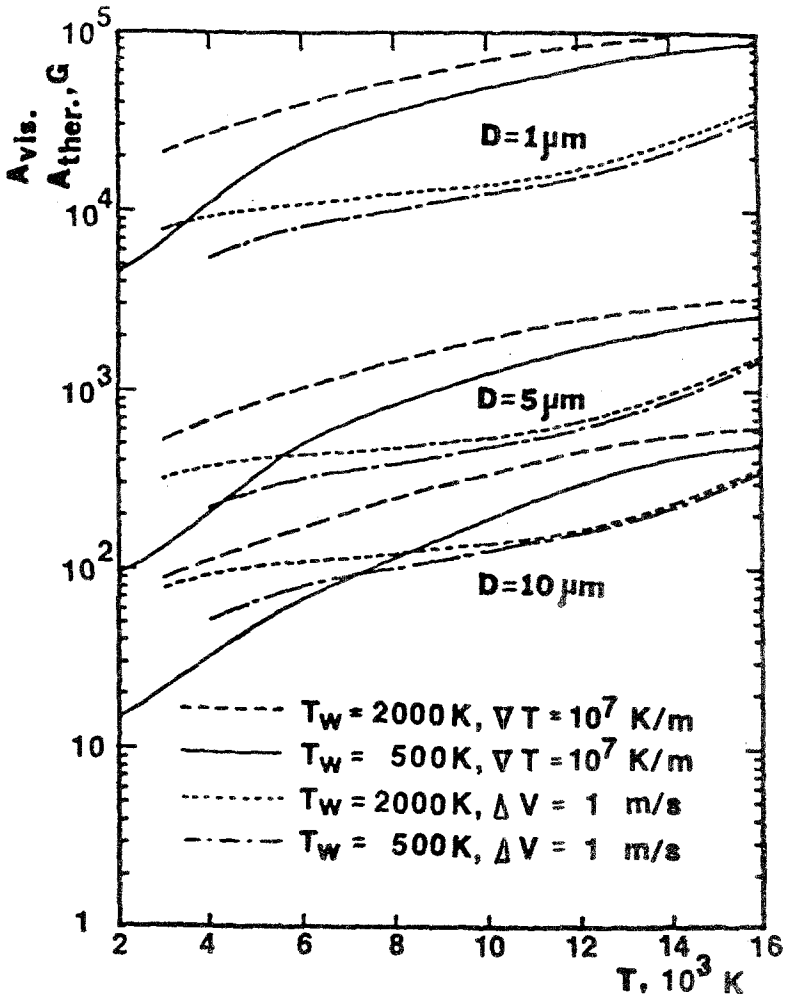


Fig. 6. Accelerations caused by viscous drag and by thermophoresis (tungsten).

These similarities can be derived from Stokian drag relations, and the former two are clearly indicated in these two figures.

3.4. Basset History Term

The local surroundings for injected particles are changing continuously in thermal plasma processing. The drag coefficient described by Eq. (7) may require additional modifications if quasisteady conditions do not

prevail. As pointed out,⁽⁸⁾ the Basset history term may modify the equation of motion under strongly nonsteady conditions.

Results of detailed calculations⁽¹⁶⁾ show that the influence of the Basset history term is much less than the viscous drag for particle sizes $< 100 \mu\text{m}$. For larger particles and small relative velocities ($\approx 1 \text{ m/s}$), however, the influence becomes important. Such small relative velocity conditions may be experienced during the final stages of processing, and they will be particularly important for light materials treated over long distances.

3.5. Thermophoresis

There has been some speculation about the effect of thermophoresis in thermal plasma processing. Based on a review by Talbot, an expression derived by Brock has been used for describing thermophoresis over the entire range of Knudsen numbers in the case of constant properties.

Another relation applies specifically for plasmas in the free molecular flow regime.⁽¹⁹⁾ As mentioned earlier, the flow conditions around a particle injected into a thermal plasma may fall into the continuum or transitional flow regime. Due to large differences between results of continuum conditions and those for free molecular flow conditions, no universal relationship can be established, unless a reasonable interpolation between the results for these two limiting cases is feasible. Unfortunately, there is no such interpolation available referring to thermophoresis under plasma conditions. Since the free molecular regime does not apply to thermal plasma processing, thermophoresis may be taken into account by applying modified constant property expressions to thermal plasma flows.⁽¹⁶⁾

Due to the similarity between the derivations of ref. 18 and refs. 13 and 14, a so-called effective mean free path length proposed in ref. 14 will be introduced:

$$\lambda^* = \frac{2\bar{K}}{\rho_w \bar{V}_w \bar{C}_p} \text{Pr}_w \quad (10)$$

where \bar{K} is the average thermal conductivity,

$$\bar{K} = \int_{T_w}^{T_g} k dT / (T_g - T_w) \quad (11)$$

\bar{C}_p is the average specific heat,

$$\bar{C}_p = \int_{T_w}^{T_g} C_p dT / (T_g - T_w) \quad (12)$$

\bar{V}_w is the average gas velocity at the surface temperature T_w , ρ_w is the density of the plasma at T_w , $T_g - T_w$ is the temperature jump on the particle surface, and Pr_w is the Prandtl number corresponding to T_w .

The results for alumina and tungsten particles in a thermal argon plasma for a temperature gradient of 10^7 K/m are also shown in Figs. 5 and 6. The values can be easily extended to larger temperature gradients. All plasma properties (μ_g , ρ_g , and K_g) are evaluated at the film temperature. Two facts are clear from these results:

- (i) Thermophoresis is strongly related to the free stream temperature and to the particle size, and it is a weak function of the surface temperature under the present assumptions.
- (ii) The magnitude of acceleration caused by thermophoresis for smaller particle sizes may be much larger than gravity effects.

Figures 5 and 6 are intended for comparison rather than for providing examples of thermophoresis and viscous drag forces. Sometimes, thermophoresis has been overestimated in explaining some observations where flow patterns actually played a more important role than thermophoresis. Thermophoresis becomes only comparable with viscous drag if the relative velocities are small (in the order of 1 m/s). Therefore, this effect is only important for very small particles ($<10 \mu\text{m}$) which relax very quickly with the flow (i.e., follow the flow field).

Particle injection may be described in two stages. The first stage is associated with the penetration of the particles into the plasma, and the second with their relaxation. Based on the previous discussion, it is clear that thermophoresis is relatively unimportant in the penetration stage because of the high relative velocities, even though the temperature gradients may assume values in the order of 10^7 K/m. In addition, the importance of thermophoresis is also questionable during the second stage. Since the temperature gradients decrease rapidly in regions remote from the walls of the reactor, the actual displacement due to thermophoresis will be rather small during the short residence time (≈ 1 ms) which is characteristic for the second stage.

3.5. Motion of Particles in Turbulent Flows

The nature of turbulent flows, as for example, experienced in plasma spraying, is its unsteadiness. The trajectories of particles injected into a "steady" flow field as predicted by the previously discussed methods become doubtful when the flow is actually fluctuating.

Based on the plasma velocity field which is locally modified by randomly oriented turbulent eddies, dispersed trajectories of a single particle can be obtained via repeated simulations of this particle. The picture of dispersed trajectories can more than qualitatively predict the influence of turbulence on particle motion during thermal plasma processing.⁽¹⁶⁾

TEMPERATURE & VELOCITY of PLASMA REACTOR

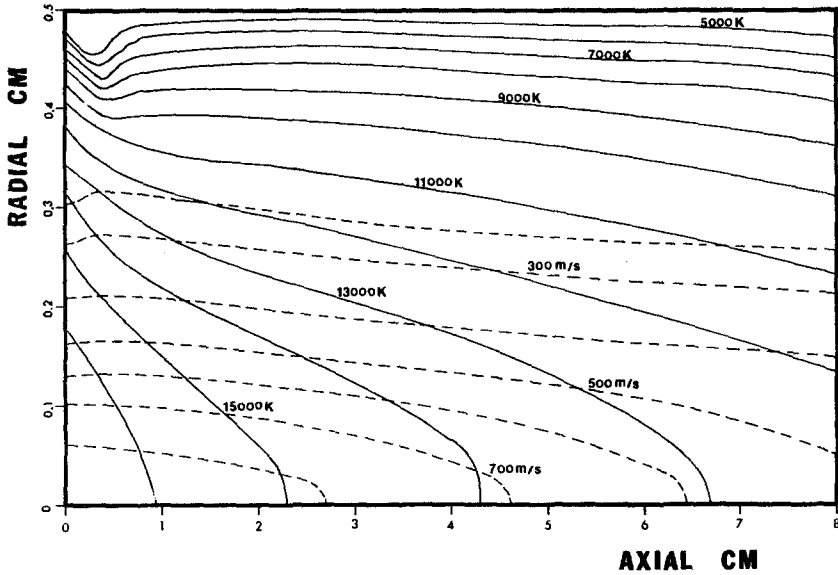


Fig. 7. Calculated temperature and velocity fields of a confined plasma jet reactor.

3.6. Results of Case Studies

Figure 7 shows calculated temperature and flow fields of a confined argon plasma jet,⁽²⁰⁾ corresponding to a plasma reactor operated in the High Temperature Laboratory of the University of Minnesota.^(11,12)

Figures 8 and 9 show typical solutions for a free turbulent argon plasma jet discharging into atmospheric air. A detailed description of the solution

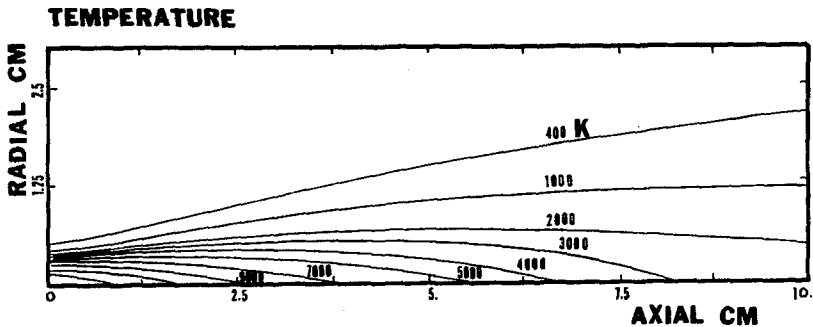


Fig. 8. Calculated temperature field of a free plasma jet reactor.

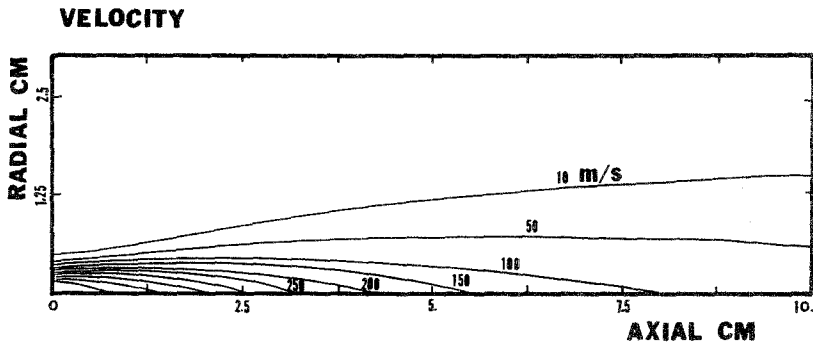


Fig. 9. Calculated velocity field of a free plasma jet reactor.

procedure for calculating these temperature and flow fields can be found in ref. 21.

Figures 10 and 11 show the trajectories of injected particles calculated under different assumptions. The calculations have been done to demonstrate the effect of various terms in the complete equation of motion.

Figure 10 shows the trajectories of $10\ \mu\text{m}$ particles injected into a confined plasma jet with a velocity of $10\ \text{m/s}$.

It is obvious that the correction term due to variable properties reduces the particle velocity, whereas noncontinuum effects seem to have little influence. Table II indicates that the additional correction term due to variable properties causes an increase of the drag coefficient from 20–40%, compared to the drag coefficients calculated with film temperatures. Therefore, it is not surprising that the predicted particle penetration into the

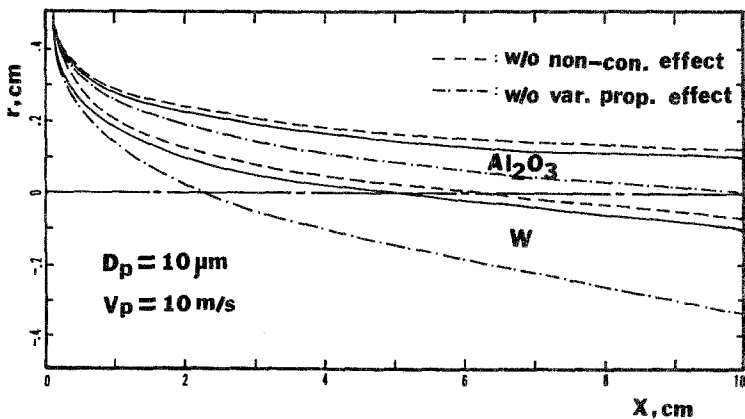


Fig. 10. Trajectories of particles injected into a confined plasma jet reactor.

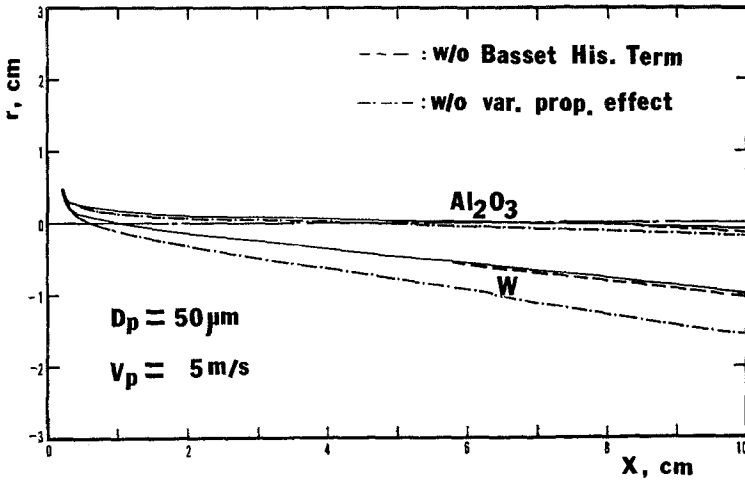


Fig. 11. Trajectories of particles injected into a free plasma jet reactor.

plasma differ substantially. On the other hand, noncontinuum effects tend to reduce the drag coefficient due to velocity slip at the surface of the particles. The Knudsen number for particles injected into the plasma is, however, small (0.05) during the early stages where the trajectory is dominated by the drag, resulting in small corrections. For smaller particle sizes ($\approx 1 \mu\text{m}$), however, this effect becomes important as shown in Fig. 4.

The effect of the Basset history term is not included in Fig. 10, because its effect is almost zero. According to the qualitative analysis in Section 3, this effect will be negligible for small particles ($\leq 10 \mu\text{m}$).

Figure 11 shows the trajectories of particles ($50 \mu\text{m}$) injected into a free plasma jet (5 m/s). The noncontinuum effect is not included, because its effect is negligible for larger particles (see Fig. 4).

The variable property effect still plays the most important role as in the case of the confined jet. The Basset history term shows a relatively small influence which becomes important for particle sizes larger than $50 \mu\text{m}$.⁽⁸⁾

For studying the effect of turbulence on particle motion, a turbulent free plasma jet has been considered with typical "eddy sizes" around 1 mm. The ranges of dispersed particle trajectories are shown in Figs. 12 and 13.

The ranges of dispersed particle trajectories are obviously larger for smaller particles ($10 \mu\text{m}$). This is due to the small mass of such particles which easily follow the motion within the eddies. It is also observed that the dispersion becomes larger downstream. This is caused by the accumulated "random walk" influence. Comparing Figs. 12 and 13 with Fig. 11, it seems that the additional variable property correction in the equation of

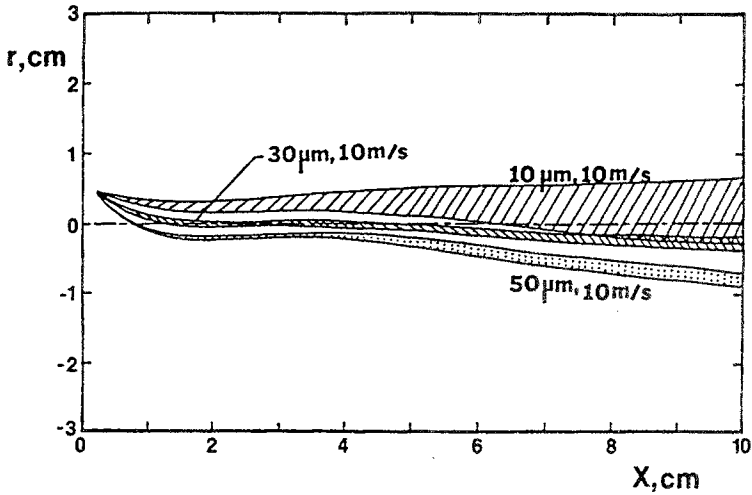


Fig. 12. Dispersed particle trajectories (alumina in plasma jet).

motion may still exceed the influence of turbulence, provided larger particles are considered. For a discussion of other effects (particle shape, evaporation, particle charging, etc.), which may influence the motion of particles in thermal plasmas, the reader is referred to refs. 16 and 21.

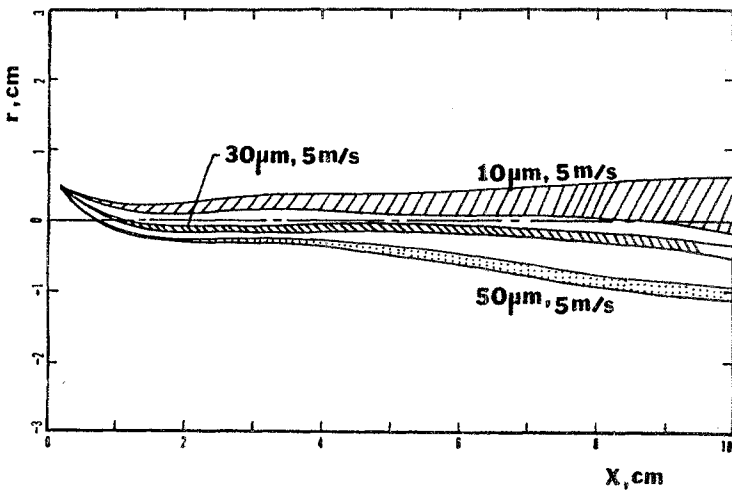


Fig. 13. Dispersed particle trajectories (tungsten in plasma jet).

Table III. Effects Involved in Particle Heat and Mass Transfer in a Thermal Plasma

-
1. Unsteady condition
 2. Modified transfer coefficients due to strongly varying plasma
 3. Vaporization and evaporation
 4. Noncontinuum effects
 5. Radiation
 6. Internal conduction
 7. Particle shape
 8. Particle charging
 9. Combination of above effects
-

4. HEAT AND MASS TRANSFER BETWEEN PARTICLES AND THERMAL PLASMAS

The various effects which may influence heat and mass transfer between particles and thermal plasmas which are known today are listed in Table III.

4.1. General Considerations

For a spherical particle with symmetric boundary conditions, heat transfer within the particle is described by the conduction equation, i.e.,

$$\rho_p C_p \frac{\partial T}{\partial t} = \frac{1}{r^2} \frac{\partial}{\partial r} \left(K_p r^2 \frac{\partial T}{\partial r} \right) \quad (13)$$

where r is the radial distance from the center of the particle, ρ_p , C_p , and K_p are the density, specific heat, and thermal conductivity of the particle, respectively.

The following effects imposed by the plasma environment on the particle have to be considered.

4.2. Convective Heat Transfer

Convective heat transfer is described by the simple equation

$$q_{\text{conv}} = h(T_\infty - T_w) \quad (14)$$

where h is the convective heat transfer coefficient, T_∞ is the surrounding plasma temperature, and T_w is the surface temperature of the particle. The convective heat transfer coefficients may be derived from semiempirical correlations. For a medium with constant properties one finds

$$\text{Nu} = \frac{hD_p}{K_p} = 2.0 + 0.6 \text{Re}^{1/2} \text{Pr}^{1/3} \quad (15)$$

where D_p is the particle diameter, Nu the Nusselt number, Re the Reynolds number, and Pr the Prandtl number. A number of corrections are needed to make this correlation compatible with the plasma environment. These corrections will be discussed later in this section.

4.3. Radiative Heat Transfer

This heat transfer mechanism refers to radiation emitted by a particle, i.e.,

$$q_{\text{rad}} = \varepsilon \sigma T_w^4 \quad (16)$$

where σ is the Stephan-Boltzmann constant, and ε the emissivity.

4.4. Vaporization of a Particle

Vaporization is defined as a mass loss process at temperatures below the boiling point. As the temperature of the particle increases, its vapor pressure increases also, leading to mass losses by vaporization, i.e.,

$$\dot{m} = \rho h_m M \ln \left(\frac{p}{p - p_v} \right) \quad (17)$$

where M is the molecular weight of the particle material, h_m the mass transfer coefficient, p the partial vapor pressure with respect to saturation, and p_v the partial vapor pressure with respect to the surface temperature of the particle. The mass transfer coefficient can be derived from a correlation similar to Eq. (15), based on an analogy between mass and heat transfer, i.e.,

$$\text{Sh} = \frac{h_m D_p}{\mathcal{D}} = 2.0 + 0.6 \text{Re}^{1/2} \text{Sc}^{1/3} \quad (18)$$

where Sh is the Sherwood number, Sc the Schmidt number, and \mathcal{D} the interdiffusivity.

4.5. Evaporation

If the surface of a particle reaches the boiling point, evaporation will take place which may be described by

$$\dot{m} = q_{\text{net}} / L_e \quad (19)$$

where L_e is the latent heat of evaporation and q_{net} the net heat transfer to the evaporating particle.

In the following, boundary conditions will be specified for the previously mentioned heat and mass transfer relationships.

4.6. Boundary Conditions (Convection and Radiation Boundary Conditions)

From an energy balance follows

$$K_p \left. \frac{\partial T}{\partial r} \right|_{r=r_0} = h(T_\infty - T_w) - \varepsilon \sigma T_w^4 \quad (20)$$

where r_0 is the radius of the particle.

4.7. Interface Between Two Phases

The interface between the solid and the liquid phase may be described by

$$K_p \left. \frac{\partial T}{\partial r} \right|_{r=r_i^-} = K_p \left. \frac{\partial T}{\partial r} \right|_{r=r_i^+} + \rho L_f \frac{dr_i}{dt} \quad (21)$$

and

$$T_i = T_{\text{melting}}$$

where r_i is the radius of the interface, and L_f the latent heat of fusion.

4.8. Diffusion Boundary of Vaporizing Particle ($T < T_{\text{boiling}}$)

This boundary condition may be described by

$$K_p \left. \frac{\partial T}{\partial r} \right|_{r=r_0} = h(T_\infty - T_w) - \varepsilon \sigma T_w^4 - \rho h_m M L_e \ln \left(\frac{p}{p - p_v} \right) \quad (22)$$

4.9. Intense Evaporation Boundary Condition for a Particle

In this case, the balance equation may be written as

$$K_p \left. \frac{\partial T}{\partial r} \right|_{r=r_0} = h(T_\infty - T_w) - \varepsilon \sigma T_w^4 + \rho L_e \frac{dr_0}{dt} \quad (23)$$

and

$$T_w = T_{\text{boiling}}$$

In addition, one more symmetry boundary condition is needed, i.e.,

$$\left. \frac{\partial T}{\partial r} \right|_{r=0} = 0$$

And, the initial condition is $T_{t=0} = T_{\text{carrier gas}}$.

The governing equations with the associated boundary conditions can be solved by numerical methods. In addition, for particulate matter with

high thermal conductivities, such as metals, the governing equations can be further simplified. By assuming that the thermal conductivity is infinite inside the particle, a uniform temperature field results for the interior of the particle.⁽²²⁾

The effects listed in Table II will affect the governing equations as well as the boundary conditions. Their relative importance for heat and mass transfer will be discussed in the following. Details of the approximations suggested by various authors may be found in ref. 21.

4.10. Variable Property Effects

Figure 14 indicates that all approximations, except that of ref. 23, produce similar results for relatively low plasma temperatures. Figures 15 and 16 show that for $T_{\infty} \geq 10^4$ K where ionization becomes important, the results of ref. 24 depart from the other results due to changes of the specific heat at higher temperatures.

In every case, the results of ref. 23 show the highest values. Even though their method is exactly fitted to the case of conduction only,⁽²⁵⁾ the reason for the large departure from all the other results is not obvious at this time.

Although the results of ref. 24 have been fitted to the data derived from computer simulations, there is no claim that this method is superior to the others, because the computer simulation has been restricted to an argon plasma.

The analysis for the mass transfer situation is quite similar to the heat transfer case and, therefore, it will not be repeated here.

From the previous discussion it is obvious that large discrepancies exist among various approaches for calculating heat transfer coefficients. This finding already indicates the need for further studies, especially for particle heat and mass transfer under various plasma conditions in order to develop reliable relationships. At present, there are almost no experimental data available. Thus, computer simulation of the plasma flow over a sphere remains an important tool for determining heat transfer coefficients.

4.11. Radiation Transport

Radiative heat transfer has been discussed extensively for particles immersed into a thermal plasma.⁽²⁵⁻²⁹⁾ For low particle loading rates, radiation from the plasma to the particles may be neglected, as well as radiative exchange among particles. Radiative heat losses from particles, however, are frequently taken into account in modeling work.^(24,30,31)

Radiative heat transfer becomes important for the following three cases:⁽²⁹⁾ (a) large particles, (b) high surface temperature and high

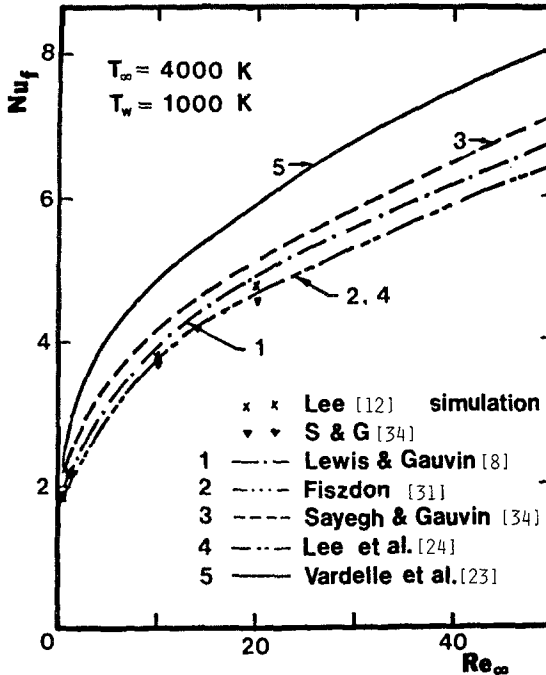


Fig. 14. Nusselt numbers derived by different authors and by computer simulation.

emissivities of the particles, and (c) low enthalpy differences between the surfaces of particles and the plasma. Radiation losses from particles are negligible except for particles with surface temperatures exceeding 2000 K immersed into plasmas (e.g., argon or nitrogen) at temperatures below 4000 K.⁽²⁵⁾

For high particle loading rates, radiation exchange among particles becomes important. In this case, the radiation field produced by emitting/absorbing particles in the plasma is no longer optically thin, and radiation absorbed by a particle may be substantial. Unfortunately, little is known for this particular situation.

4.12. Internal Conduction

Internal conduction within a particle in a thermal plasma may lead to large differences between the surface and the center temperature of a particle. The Biot number, defined as the ratio of convective to conductive heat transfer, serves as a criterion for determining the relative importance of heat conduction within a particle. If $Bi \ll 0.1$, internal conduction is relatively

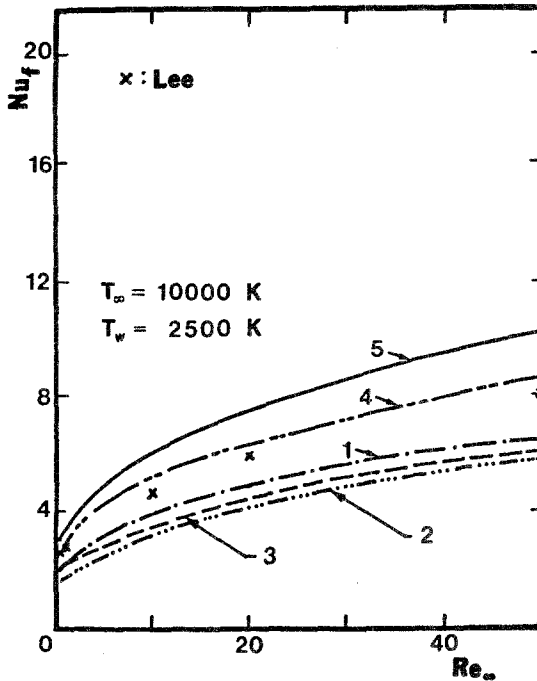


Fig. 15. Nusselt numbers derived by different authors and by computer simulation. (Number and symbol identification are the same as in Fig. 14.)

high (i.e., temperature variations within the particle are negligible). For particles immersed into thermal plasmas, this criterion depends heavily on the material of the particle and on the thermal conductivity of the plasma. Bourdin *et al.*⁽²⁵⁾ proposed a method for calculating the Biot number assuming that conduction is the governing heat transfer mechanism (small Reynolds numbers) for particle heating in the plasma. They found that the difference between the surface and center temperature of a particle becomes less than 5% of the difference between the plasma and the surface temperature of a particle if $Bi < 0.02$.

Based on this criterion the internal conduction resistance of the particle is negligible if $Bi_{crit} \ll 1$. For this case, a simplified approach can be used to calculate heat and mass transfer.⁽²²⁾

4.13. Vaporization and Evaporation

Vaporization and evaporation are physical processes concerned with mass transfer across a liquid-vapor interface. Vaporization is defined as a mass transfer process driven by vapor concentration gradients existing

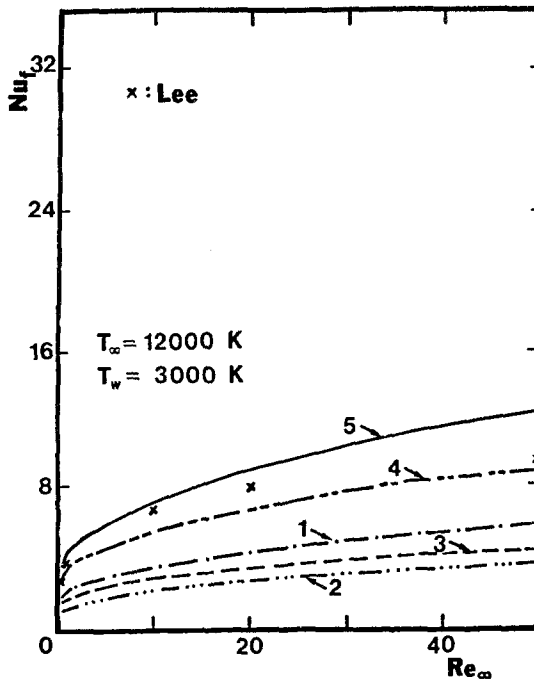


Fig. 16. Nusselt numbers derived by different authors and by computer simulation. (Number and symbol identification are the same as in Fig. 14.)

between the free stream and the particle surface. In contrast, evaporation accounts for large amounts of mass transfer as the surface temperature reaches the boiling point.

At the interface between liquid and vapor phases, a heat balance is maintained and at the same time a bulk flow of material crosses the interface. For high mass transfer rates, the transfer coefficients become functions of the mass transfer rate, thus causing nonlinearities in the transport equations. For example, in ref. 32 it has been shown that the heat flux through a liquid-vapor interface is reduced due to the absorption of heat by the vapor. This, however, does not invalidate the definitions of the transfer coefficients.

Numerical simulation of a particle residing in a high-temperature surrounding has been performed based on the model described in ref. 12. The noncontinuum effect which will be discussed in the next section has been included. Two limiting cases for vaporization can be established. For Case I, no mass vaporization (or mass diffusion) is taken into account⁽²²⁾ before the particle surface reaches the boiling point. In Case II the vaporization rate driven by the vapor pressure is determined by Eq. (17).^(30,33)

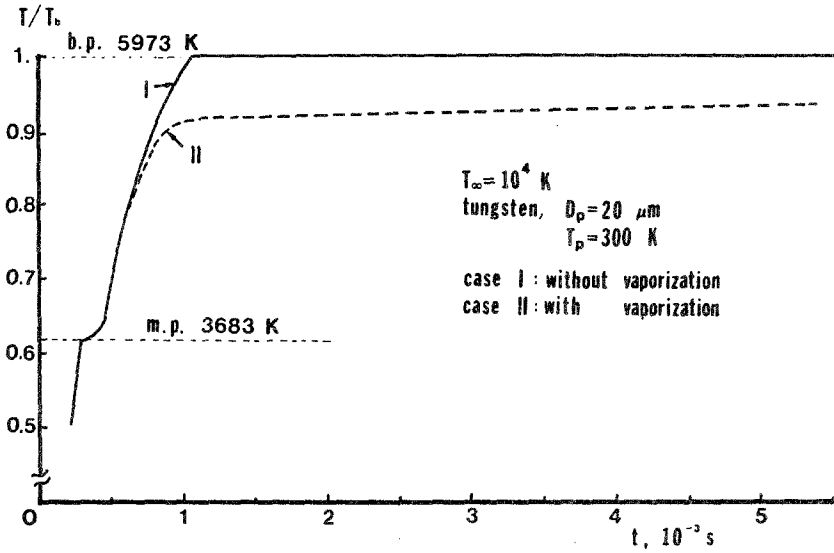


Fig. 17. Normalized temperature history of vaporization and evaporation. (Note: in Case I evaporation starts as the particle surface reaches the boiling point.)

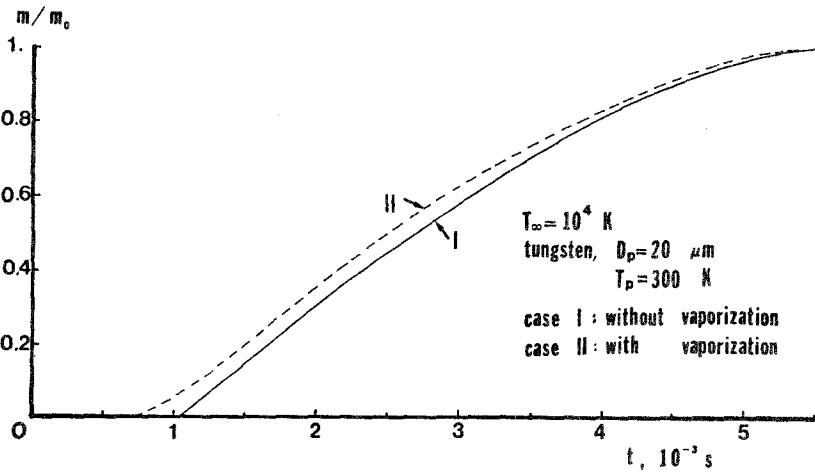


Fig. 18. Normalized total mass transfer from a particle (m_0 = initial mass of the particle).

The results of corresponding calculations are presented in Figs. 17 and 18. In Fig. 17 normalized temperatures are plotted as a function of time after the particle has been exposed to a thermal plasma. Particular attention is focused on the region where vaporization or evaporation occurs. Figure 12 indicates that the surface temperature reaches a "plateau" (Case II) at some temperature below the boiling point and continues to rise very slowly. For Case I, there is no vaporization before the surface temperature reaches the boiling point. The results of Fig. 18 show that the total mass transfer through the interface is almost the same for both cases, which is an important finding. Additional studies have shown that the differences between the two limiting cases becomes less significant for higher free stream temperatures and/or lower boiling point materials.

These results can be explained in terms of the relatively high free stream temperature compared to the surface temperature of a particle. The heat input from the surroundings to a particle is governed by the temperature difference between the surroundings and the particle surface. This temperature difference is little affected by possible variations of the particle surface temperature. Consequently, the total heat input is not sensitive to the particle surface temperature. Hence, the total mass transfer curves show little sensitivity to the different mechanisms or different surface temperatures. This result reveals that the choice of the equation for calculating vaporization rates is not critical for this interphase mass transfer process.

It is felt that the results shown in Figs. 17 and 18 should provide an interpretation of the long-standing puzzle about heat and mass transfer through a liquid-vapor interface. A final settlement of this controversy must await experimental verification of these predictions.

4.14. Noncontinuum Effects

As mentioned previously, the particle sizes used for plasma processing may be of the same order of magnitude as the molecular mean free path lengths in the plasma. This "rarefaction effect" may exert a strong influence on heat transfer.

The noncontinuum effect on heat transfer has been studied in ref. 13 in the temperature jump regime, resulting in a proposed correction:

$$\frac{q_{\text{noncont}}}{q_{\text{cont}}} = \frac{1}{1 + (Z^*/r_p)} \quad (24)$$

where Z^* is the jump distance.

The noncontinuum effect becomes substantial for small particles. Therefore, it is crucial for modeling associated with thermal plasma processing⁽²⁰⁾ when small particles (<20 μm) are involved. The approach used in ref. 20

is based on the so-called temperature jump which is valid for Knudsen numbers in the range $0.001 < \text{Kn} < 1$.

Substantially more work is needed to clarify the effects of particle shape and particle charging on heat and mass transfer. Some discussion about these effects is included in ref. 21.

5. SUMMARY AND CONCLUSIONS

The results related to momentum transfer indicate that (i) the correction term required for the viscous drag coefficient due to strongly varying properties is the most important factor; (ii) noncontinuum effects is the most important factor; (ii) noncontinuum effects are important for particle sizes $< 10 \mu\text{m}$ at atmospheric pressure and these effects will be enhanced for smaller particles and/or reduced pressures; (iii) the Basset history term is negligible, unless relatively large and light particles are considered over long processing distances; (iv) thermophoresis is not crucial for the injection of particles into thermal plasmas; (v) turbulent dispersion becomes important for particles $< 10 \mu\text{m}$ in diameter.

Results associated with heat and mass transfer show that (i) convection heat transfer coefficients require extensive modification due to strongly varying plasma properties; (ii) vaporization, defined as a mass transfer process corresponding to particle surface temperatures below the boiling point, describes a different particle heating history than that of the evaporation process which, however, is not a critical control mechanism for interphase mass transfer of particles in thermal plasmas.

ACKNOWLEDGMENTS

This work has been supported by the National Science Foundation under grant NSF/CPE 82000628. The contributions of Drs. Y. C. Lee and Y. P. Chyou are gratefully acknowledged.

REFERENCES

1. H. Maecker, *Z. Phys.* **141**, 198 (1955).
2. P. J. Shayler and M. T. C. Fanz, *J. Phys. D: Appl. Phys.* **10**, 1659.
3. J. Mostaghimi-Tehrani and E. Pfender, *Plasma Chem. Plasma Process.* **4**, 129 (1984).
4. D. M. Chen and E. Pfender, *IEEE Trans. Plasma Sci.* **PS-9**, 4, 265 (1981).
5. E. Pfender, in *Gaseous Electronics*, Vol. 1, Academic Press, New York (1978).
6. R. Clift, J. R. Grace, and M. E. Weber, *Bubbles, Drops and Particles*, Academic Press, New York (1978).
7. C. T. Crowe, in *Pulverized Coal Combustion and Gasification*, L. D. Smoot and D. T. Pratt, eds., Plenum, New York (1979), p. 107.
8. J. A. Lewis and W. H. Gauvin, *AIChE J.* **19**, 982 (1973).

9. C. Sheer, S. Korman, D. J. Angier, and R. P. Cahn, in *Fine Particles*, W. E. Kuhn, ed., 2nd International Conference, The Electrothermics Metallurgy Div., Electrochemical Society, Boston, Massachusetts (1974).
10. F. M. White, *Viscous Fluid Flow*, McGraw-Hill, New York (1974).
11. Y. C. Lee, K. C. Hsu, and E. Pfender, *5th International Symposium on Plasma Chemistry* **2**, 795 (1981).
12. Y. C. Lee, Trajectories and Heating of Particles Injected into a Thermal Plasma, Master thesis, Department of Mechanical Engineering, University of Minnesota (1982).
13. X. Chen and E. Pfender, *Plasma Chem. Plasma Process.* **3**, 97 (1983).
14. X. Chen and E. Pfender, *Plasma Chem. Plasma Process.* **3**, 351 (1983).
15. W. F. Phillips, *Phys. Fluids* **18**, 1089 (1975).
16. Y. C. Lee and E. Pfender, *Plasma Chem. Plasma Process.* **5**, 3 (1985).
17. L. Talbot, in *Rarefied Gas Dynamics*, Vol. 74, S. S. Fisher, ed., AIAA Book (1981), p. 467.
18. J. R. Brock, *J. Colloid Sci.* **17**, 768 (1962).
19. J. R. Brock, *Nature* **204**, 69 (1964).
20. X. Chen, Y. C. Lee, and E. Pfender, *6th International Symposium on Plasma Chemistry* **1**, 51 (1983).
21. Y. C. Lee, Modeling Work in Thermal Plasma Processing, Ph.D. thesis, Department of Mechanical Engineering, University of Minnesota (1984).
22. M. I. Boulos, *IEEE Trans. Plasma Sci.* **4**, 93 (1978).
23. M. Vardelle, A. Vardelle, P. Fauchais, and M. I. Boulos, *AIChE J.* **29**, 236 (1983).
24. Y. C. Lee, K. C. Hsu, and E. Pfender, *Fifth International Symposium on Plasma Chemistry* **2**, 795 (1981).
25. E. Bourdin, P. Fauchais, and M. I. Boulos, *Int. J. Heat Mass Transfer* **26**, 567 (1983).
26. B. Waldie, *The Chemical Engineer* **May**, 188 (1972).
27. C. Bonet, M. Daguene, and M. Dumargue, *Int. J. Heat Mass Transfer* **17**, 643 (1974).
28. C. Bonet, M. Daguene, and M. Dumargue, *Int. J. Heat Mass Transfer* **17**, 1559 (1974).
29. X. Chen and E. Pfender, *Plasma Chem. Plasma Process.* **2**, 293 (1982).
30. T. Yoshida and K. Akashi, *J. Appl. Phys.* **48**, 2252 (1977).
31. J. K. Fizsdon, *Int. J. Heat Mass Transfer* **22**, 749 (1979).
32. X. Chen and E. Pfender, *Plasma Chem. Plasma Process.* **2**, 185 (1982).
33. F. J. Harvey and T. N. Meyer, *Metallurgical Trans. B* **9B**, 615 (1978).
34. N. N. Sayegh and W. H. Gauvin, *AIChE J.* **25**, 522 (1979).